Excited-State Double-Proton Transfer in the 7-Azaindole Dimer in the Gas Phase. 2. Cooperative Nature of Double-Proton Transfer Revealed by H/D Kinetic Isotopic Effects

Kenji Sakota and Hiroshi Sekiya*

Department of Chemistry, Faculty of Sciences, Kyushu University, 6-10-1 Hakozaki, Higashi-ku, Fukuoka 812-8581, Japan

Received: September 17, 2004; In Final Form: December 27, 2004

The dispersed fluorescence (DF) spectra of the 7-azaindole dimer ($7AI_2$) and deuterated dimers $7AI_2$-*hd* and $7AI_2$-*dd*, where *hd* and *dd* indicate the deuteration of an imino proton and two imino protons, have been measured in a supersonic free jet expansion. The undeuterated $7AI_2$-*hh* dimer exhibits only the tautomer fluorescence, but both the normal and tautomer fluorescence have been detected by exciting the origins of $7AI_2$-*h*d*, $7AI_2$-*hd** and $7AI_2$-*dd* in the S_1-S_0 region, where *h** and *d** indicate the localization of the excitation on 7AI-*h* or 7AI-*d* moiety. The DF spectra indicate that $7AI_2$-*h*d* and $7AI_2$-*hd** undergo excited-state proton/deuteron transfer (ESPDT), while excited-state double-deuteron transfer (ESDDT) occurs in $7AI_2$-*dd*. The H/D kinetic isotopic effects on ESDPT have been investigated by measuring the intensity ratios of the normal fluorescence to the tautomer fluorescence. The ESPDT rate is about 1/60th of the ESDPT rate, and the ESDDT rate is about 1/12th of the ESPDT rate, where ESPDT rate is an average of the rates for $7AI_2$-*h*d* and $7AI_2$-*hd**. The observed H/D kinetic isotope effects imply that the ESDPT reaction of $7AI_2$ has a "*cooperative*" nature; i.e., the motion of the two moving protons strongly couples each other through the electron motions. The difference in the estimated ESPDT reaction rates, 9.8×10^9 and 6.9×10^9 s^{-1} for $7AI_2$-*h*d* and $7AI_2$-*hd**, respectively, is consistent with the concerted mechanism rather than the stepwise mechanism.

Introduction

The proton transfer reaction in hydrogen-bonded systems has been a subject of numerous spectroscopic and theoretical studies, not only because it involves the quantum mechanical tunneling process but also because it plays a crucial role in many chemical and biological processes. The doubly hydrogen-bonded 7AI dimer ($7AI_2$) is a prototypical system that exhibits the excited-state double-proton transfer (ESDPT) and has been recognized as a simple model molecule of the hydrogen-bonded DNA base pairs. The investigation of the reaction mechanism of ESDPT in $7AI_2$ may provide information about the mutation of DNA induced by UV irradiation.

Since the first observation of ESDPT in $7AI_2$ by Kasha et al., many experimental and theoretical studies have been reported.[1−20] The time-resolved studies on $7AI_2$ with femtosecond resolution have concentrated on whether the two protons translocated in a concerted way (concerted mechanism) or in a stepwise way (stepwise mechanism) in the ESDPT reaction.[8,12−14] Douhal et al. observed biexponential decay signals with fast components of 200−650 fs and slow components of 1.6−3.3 ps with the femtosecond time-resolved pump−probe mass spectrometry.[8] They assigned the fast component to the first proton transfer and the slow component to the second proton transfer. On the basis of these data the stepwise mechanism was proposed for the ESDPT reaction in $7AI_2$. Essentially the same conclusion was obtained from a femtosecond time-resolved Coulomb explosion technique.[13]

Very recently, we have measured the UV−UV hole-burning spectra of $7AI_2$ and deuterated $7AI_2$ in a supersonic free jet expansion.[18] The vibronic bands are well separated in the deuterated dimers due to the narrowing of the bandwidths. This enabled us to provide unambiguous assignments for the vibronic bands. We suggested that the biexponential decay profiles in the femtosecond time-resolved study result from the excitations of closely spaced vibronic bands having different lifetimes arising from vibrational mode-selective ESDPT.[5] Thus, the observation of biexponential decay profiles by Douhal et al. shows no direct evidence of the stepwise mechanism.[18]

The dispersed fluorescence (DF) spectrum of the deuterated $7AI_2$ was measured in the low-temperature matrix.[19] In this spectrum, fluorescence from the normal form of the deuterated $7AI_2$ was observed, but the tautomer fluorescence was absent. On the basis of this observation, the authors concluded that the ESDDT in the deuterated $7AI_2$ is blocked at low temperature. However, El-Bayoumi et al. had observed dual fluorescence from the deuterated $7AI_2$ dimer in 3-methylpentane at 77 K with time-resolved spectroscopy.[21] Femtosecond and picosecond time-resolved fluorescence spectroscopy at room temperature in the condensed phase showed that the time constants are similar for the undeuterated and deuterated $7AI_2$ dimers: $\tau \approx 1$ ps for the undeuterated $7AI_2$ and $\tau \approx 2-5$ ps for the deuterated $7AI_2$.[6,12,14] Thus, the observed H/D kinetic isotope effect on the ESDPT reaction in $7AI_2$ is inconsistent between authors; therefore, the measurements of the vibronic state-selected kinetic isotope effects in a supersonic molecular beam are desirable. It is very important to investigate the accurate kinetic isotope effects on ESDPT for $7AI_2$ in order to understand the dynamics of the ESDPT reaction. Douhal et al. measured the decay profiles of the deuterated $7AI_2$ as well as those of the undeuterated $7AI_2$ in a supersonic molecular beam.[8] However, it is difficult to select the vibronic states of $7AI_2$ with the ultrashort femtosecond pulse, as suggested by the UV−UV hole-burning spectra.[18]

* To whom correspondence should be addressed. E-mail: hsekiscc@mbox.nc.kyushu-u.ac.jp.

10.1021/jp045772m CCC: $30.25
Published on Web 03/04/2005

SCHEME 1

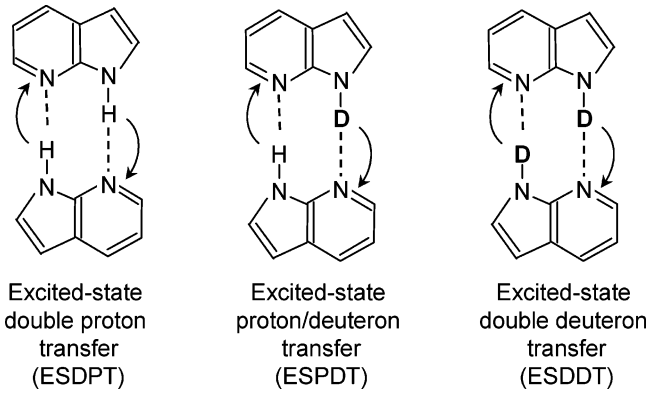

We have shown that the excitation is completely localized in one monomer unit in the S_1 state of $7AI_2$-*hd*;[25] therefore it is possible to measure the DF spectra of $7AI_2$-*h*d* and $7AI_2$-*hd** separately by exciting the vibronic bands of each species. The measurement of the normal fluorescence and the tautomer fluorescence by exciting a single vibronic state may provide crucial information on the ESDPT dyamics. In the present work, we report the first observation of the DF spectra of jet-cooled $7AI_2$-*hd* and $7AI_2$-*dd*, where *hd* and *dd* indicate that one of the imino hydrogen (N−H) and the two imino hydrogens are deuterated, respectively. Dual fluorescence has been observed in the DF spectra of $7AI_2$-*hd* and $7AI_2$-*dd*, respectively, indicating that excited-state proton and deuteron transfer (ESPDT) or double-deuteron transfer (ESDDT) occurs in these species (Scheme 1). The measurement of the relative intensity ratios of the normal dimer fluorescence to the tautomer fluorescence for $7AI_2$-*hd* and $7AI_2$-*dd* provides vibronic state-selected *hh*/*h*d*/*hd**/*dd* kinetic isotope effects on the ESDPT reaction. Prominent H/D kinetic isotope effects have been observed. We discuss the ESDPT dynamics in $7AI_2$ on the basis of the kinetic isotope effects.

Experimental Procedures

The experimental apparatus used for the fluorescence excitation (FE) spectra of the $7AI_2$ dimers has been described in part 1[25] and the literature.[26] We briefly describe about the dispersed fluorescence (DF) spectroscopy. The DF spectra were measured by using a frequency-doubled dye-laser (Lumonics HD-300 and Lumonics HT-1000) pumped by a second harmonic of the Nd^{3+}:YAG laser (Spectra Physics GCR 230). A single monochromator (Spex 1704) was used to measure the dispersed fluorescence spectra. The dispersed fluorescence was detected by a photomultiplier (Hamamatsu R955). Because the detection sensitivity of the monochromator including the photomultiplier and focusing lenses is different in each wavelength, the calibration of the detection sensitivity was carried out with a halogen lamp (USIO Inc. JPD-100-500CS). The vertical axis of the dispersed fluorescence spectrum in this paper corresponds to the relative photon number. 7AI was purchased from TCI and was used without purification. Deuterated $7AI_2$ were produced by introducing a few drops of D_2O into the nozzle housing.

Results

Figure 1 shows the FE spectrum of a mixture of the undeuterated and deuterated $7AI_2$ in the $1B_u$-$1A_g$ or $2A'$-$1A'$ region measured by monitoring visible emission with a Y45 filter. The vibronic bands detected in this spectrum are definitely assigned by the UV−UV hole-burning spectroscopy.[18] We clearly observed the origins and intermolecular vibrations of four isotopomers, $7AI_2$-*hh*, $7AI_2$-*h*d*, $7AI_2$-*hd**, and $7AI_2$-*dd* in Figure 1. It should be noted that the lowest excited states of $7AI_2$-*hh* and $7AI_2$-*dd* can be explained by a weak coupling case of the exciton model;[22−25] i.e., the excitation is *delocalized* on the dimer. In contrast, the excitation is *localized* on a half unit of $7AI_2$-*h*d* or $7AI_2$-*hd** in the lowest excited state of $7AI_2$-*hd* and the separation of the two origins is 21 cm^{-1};[18,25] therefore each monomer unit can be distinguished in $7AI_2$-*hd* and separately excited with a UV laser.

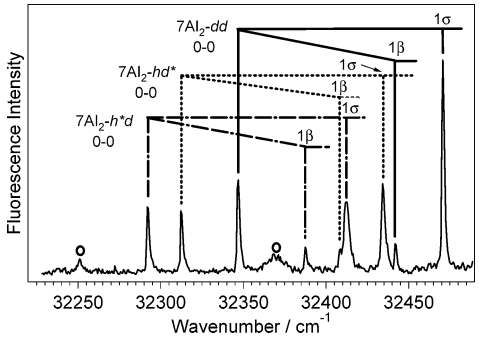

Figure 1. FE spectrum of a mixture of the undeuterated and deuterated $7AI_2$ in a supersonic free jet expansion. The open circles indicate the transition due to $7AI_2$-*hh*. Two transitions separated by 21 cm^{-1} are detected in the spectrum of $7AI_2$-*hd* due to the localization of the excitation on the 7AI-*h* or 7AI-*d* moiety; the two localized dimers are denoted by $7AI_2$-*h*d* and $7AI_2$-*hd**, respectively.

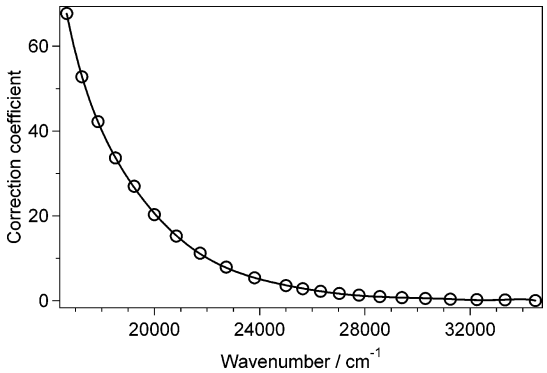

Figure 2. Calibration curve used for the correction of the fluorescence intensity. The calibration curve was obtained by comparing the spectral irradiance of the standard halogen lamp to the actual signal intensity detected with the photomultiplier. The experimentally obtained coefficients and the curve fitted with polynomial functions are indicated by the open circles and the solid line, respectively.

Figure 2 shows the calibration coefficient versus wavenumber to correct the detection sensitivity of the optical system including the monochromator, photomultiplier, and focusing lenses. This curve was obtained by comparing the spectral irradiance of the standard halogen lamp to the photosignal detected with the photomultiplier and the digital oscilloscope. Very low detection sensitivity in the visible region is mainly due to both the low diffraction efficiency of a grating brazed at 300 nm and the low sensitivity of the photomultiplier. Thus, we obtained the DF spectra where the intensity of fluorescence is converted to the relative photon numbers by calibrating the uncorrected DF spectra.

In Figure 3, we show the uncorrected and corrected DF spectra of $7AI_2$-*h*d* and $7AI_2$-*hd**, respectively. The DF spectra of $7AI_2$-*h*d* or $7AI_2$-*hd** are indicated by the broken and solid lines, respectively. The intensity distributions in the corrected spectra are very different from those of the uncorrected DF

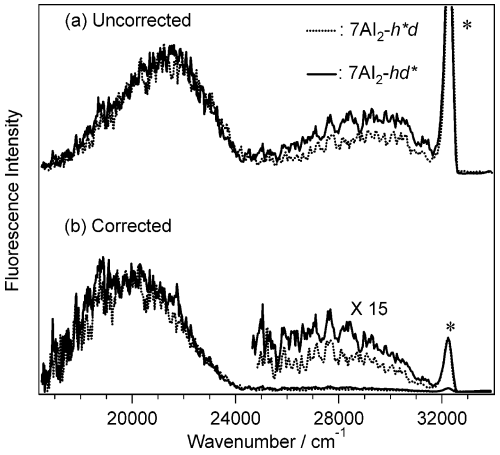

Figure 3. Uncorrected (a) and corrected (b) DF spectra of $7AI_2$-*h*d* and $7AI_2$-*hd**. The DF spectra of $7AI_2$-*h*d* and $7AI_2$-*hd** are indicated by the broken and solid lines, respectively. The bands marked with the asterisks contain the laser scattering light.

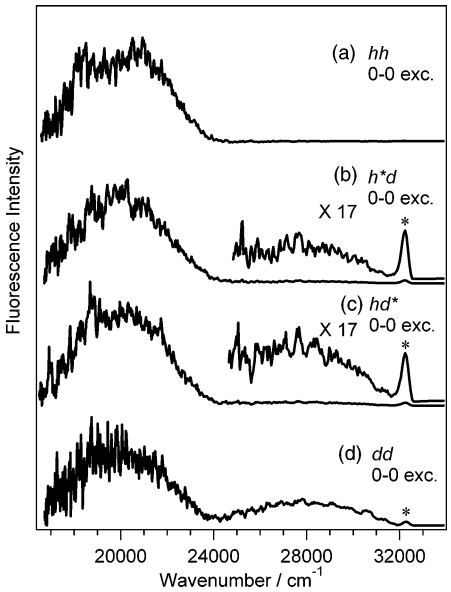

Figure 4. DF spectra of $7AI_2$-*hh* (a), $7AI_2$-*h*d* (b), $7AI_2$-*hd** (c), and $7AI_2$-*dd* (d) measured by exciting the 0−0 transitions of each dimer. The relative photon number is indicated as the intensity of fluorescence. The bands indicated by the asterisks contain the laser scattering light.

spectra. It should be noted that the fluorescence intensity of $7AI_2$-*h*d* is clearly different from that of $7AI_2$-*hd** in the UV region both in the corrected and uncorrected DF spectra. This result indicates that there is significant difference in the ESPDT rates for $7AI_2$-*h*d* and $7AI_2$-*hd**.

Figure 4 shows the corrected DF spectra of four isotopomers following the excitation of the origin bands. In Figure 4a, fluorescence from the tautomer of $7AI_2$-*hh* is observed in the visible region, whereas fluorescence from the normal dimer in the UV region is absent. This result is consistent with the occurrence of rapid ESDPT reaction ($\tau_{PT} = 1.1$ps) and a very low fluorescence quantum yield (2.9×10^{-5}) for the normal dimer of $7AI_2$-*hh* measured in the condensed phase.[12] Parts b and c of Figure 4 show the DF spectra of $7AI_2$-*h*d* and $7AI_2$-*hd**, respectively. In these spectra, weak UV fluorescence from the normal dimer is detected, together with the largely Stokes-shifted tautomer fluorescence. The observation of the normal dimer fluorescence from $7AI_2$-*h*d* and $7AI_2$-*hd** indicate that the ESPDT rates for $7AI_2$-*h*d* and $7AI_2$-*hd** are slower than the ESDPT rate for $7AI_2$-*hh*. The relative intensity ratios of the

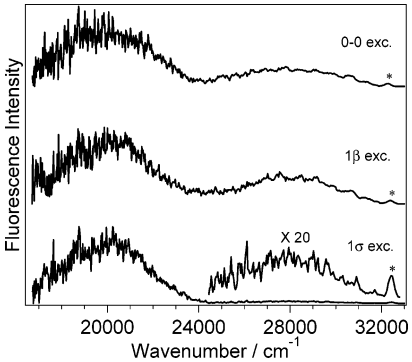

Figure 5. DF spectra of $7AI_2$-*dd* measured by exciting the transitions to the zero-point level and intermolecular vibrations 1β and 1σ. The relative photon number is indicated as the intensity of fluorescence. The bands indicated by the asterisks contain the laser scattering light.

normal dimer fluorescence to the tautomer fluorescence are different between $7AI_2$-*h*d* and $7AI_2$-*hd**, respectively; the normal dimer fluorescence is more strongly observed in $7AI_2$-*hd** than in $7AI_2$-*h*d*. Figure 4(d) shows the DF spectrum of $7AI_2$-*dd*. In this spectrum, the normal dimer fluorescence is clearly observed, together with the tautomer fluorescence. The strongly observed normal dimer fluorescence of $7AI_2$-*dd* indicates that the ESDDT rate for $7AI_2$-*dd* is much slower than the ESPDT rates for $7AI_2$-*hd** and $7AI_2$-*h*d*. The reductions in the ESPDT and ESDDT rates for the deuterated $7AI_2$ dimers as compared with the ESDPT rate for the undeuterated $7AI_2$ suggest that the ESDPT of $7AI_2$ proceeds through the tunneling mechanism in the gas phase.

Figure 5 shows the DF spectra of $7AI_2$-*dd* following the excitation of the origin, intermolecular bending (1β) and stretching (1σ) vibrations. The normal dimer fluorescence is observed in these spectra, together with the tautomer fluorescence. The relative intensity ratio of the normal dimer fluorescence to the tautomer fluorescence substantially depends on the excited vibronic state. The intensity ratios are similar for the excitation of the intermolecular bending (1β) vibration and the origin. But, the intensity of the tautomer fluorescence drastically increases when the intermolecular stretching (1σ) vibration is excited, and weak normal dimer emission is also detected.

Discussion

A. Dual Fluorescence and ESDPT Rates. Dual fluorescence has been observed by the photoexcitation of $7AI_2$-*hd* and $7AI_2$-*dd* under the isolated conditions for the first time. The ESPDT and ESDDT rate constants for the deuterated $7AI_2$ dimers can be estimated from the relative intensity ratios of the normal dimer fluorescence to the tautomer fluorescence by considering a kinetic model schematically represented in Figure 6. The relative fluorescence intensity in Figures 4 and 5 is converted to the relative photon numbers; therefore the intensity ratio of the normal dimer fluorescence to the tautomer fluorescence corresponds to the relative ratio of the fluorescence quantum yields of the normal dimers (Φ^n) to the products of the quantum yield of the ESPDT (or ESDDT) reaction and the fluorescence quantum yield of the tautomers (Φ^t):

$$\frac{I(\text{normal})}{I(\text{tautomer})} = \frac{\Phi^n}{\Phi^t} \tag{1}$$

where I(normal) and I(tautomer) are the fluorescence intensities

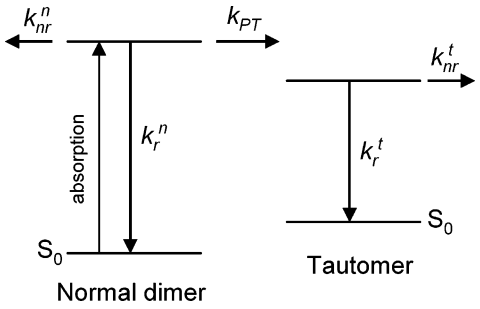

Figure 6. Energy level diagram for the normal dimer and the tautomer of $7AI_2$. $k_r^{n(t)}$ and $k_{nr}^{n(t)}$ are the rate constants for the radiative and the nonradiative decay in the normal dimer (n) and the tautomer (t), respectively, and k_{PT} denotes the ESDPT rate constant.

TABLE 1: Intensity Ratios of the Normal Dimer Fluorescence to the Tautomer Fluorescence, and the ESDPT, ESPDT, and ESDDT Rate Constants

species	I(normal)/I(tautomer)	k_{PT}/s^{-1}
$7AI_2$-*hh*	≈0	[a]
$7AI_2$-*h*d*	0.029 ± 0.002[b]	$(9.8 \pm 0.6) \times 10^9$
$7AI_2$-*hd**	0.042 ± 0.006[b]	$(6.9 \pm 1.1) \times 10^9$
$7AI_2$-*dd*	0.36 ± 0.05[b]	$(7.0 \pm 1.0) \times 10^8$

[a] An upper limit of the ESDPT rate constant for $7AI_2$-*hh* ($\approx 5 \times 10^{11}$ s^{-1}) has been estimated from the band shape of the origin band in the FE spectrum. [b] Experimental errors arise from the fluctuations of the detected fluorescence intensity. These errors are employed to estimate the errors in k_{PT} listed in the column of k_{PT}/s^{-1}.

of the normal dimer and the tautomer, respectively. Φ^n and Φ^t in eq 1 are expressed as follows,

$$\Phi^n = \frac{k_r^n}{k_{nr}^n + k_r^n + k_{PT}^{XX}} \tag{2}$$

$$\Phi^t = \frac{k_{PT}^{XX}}{k_{nr}^n + k_r^n + k_{PT}^{XX}} \cdot \frac{k_r^t}{k_r^t + k_{nr}^t} \tag{3}$$

where $k_r^{n(t)}$ and $k_{nr}^{n(t)}$ are the rate constants for the radiative and nonradiative decay in the normal dimer (n) and the tautomer (t), respectively. The rate constants k_{PT}^{XX} for ESDPT, ESPDT, and ESDDT are distinguished with notations k_{PT}^{hh}, k_{PT}^{hd}, and k_{PT}^{dd}. From (2) and (3), we obtain the following equation.

$$k_{PT}^{XX} = \frac{k_r^n \cdot (k_r^t + k_{nr}^t)}{k_r^t \cdot \left(\frac{\Phi^n}{\Phi^t}\right)} \tag{4}$$

The radiative lifetimes of the normal dimer and the tautomer of $7AI_2$-*hh* are determined to be $(k_r^n)^{-1} = 38$ ns and $(k_r^t)^{-1} = 160$ ns.[12] The decay profiles of the tautomer fluorescence are observed for $7AI_2$-*hh* and $7AI_2$-*dd* in 3-methypentane at 77 K.[3] These decay profiles are fitted with single exponentials ($\tau^{hh} = 13.3$ ns for $7AI_2$-*hh* and $\tau^{dd} = 16.9$ ns for $7AI_2$-*dd*), so that the observed lifetimes in ref 3 are approximately $(k_r^t + k_{nr}^t)^{-1}$. For $7AI_2$-*hd*, an average of $(k_r^t + k_{nr}^t)^{-1}$ for $7AI_2$-*hh* and $7AI_2$-*dd* is used as an approximation. With the use of these constants, the vibronic state-selective rate constants k_{PT}^{hd} and k_{PT}^{dd} for the deuterated $7AI_2$ dimers can be calculated with eq 4. The results are summarized in Tables 1 and 2. The k_{PT}^{hh} value cannot be estimated from the DF spectrum, because no normal dimer fluorescence is observed. We have obtained a k_{PT}^{hh} value from the bandwidth of the 0−0 transition in the FE spectrum, which is described in detail in section B.

TABLE 2: Intensity Ratios of the Normal Dimer Fluorescence to the Tautomer Fluorescence and the ESDDT Rate Constants Obtained by Exciting Different Vibrational Modes

vibrational mode	I(normal)/I(tautomer)	k_{PT}/s^{-1}
0−0	0.36 ± 0.05	$(7.0 \pm 1.0) \times 10^8$
1β[a]	0.46 ± 0.05	$(5.4 \pm 1.0) \times 10^8$
1σ[b]	0.042 ± 0.006	$(6.0 \pm 0.7) \times 10^9$

[a] One quantum of intermolecular bending vibration. [b] One quantum of intermolecular stretching vibration.

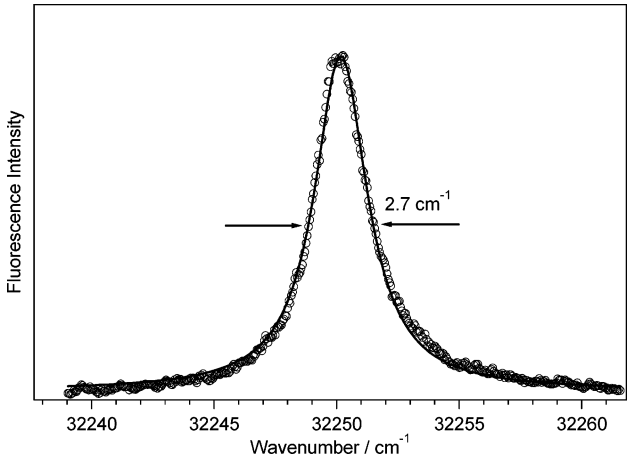

Figure 7. Experimentally obtained band envelope of the 0−0 band of $7AI_2$-*hh* (open circles) is fitted with a Lorentzian function (solid curve). The band envelope is well reproduced with fwhm = 2.7 cm^{-1}.

It is clear from Figure 5 and Table 2 that k_{PT}^{dd} remarkably depends on the excited intermolecular vibration. It was suggested that the excitation of the intermolecular stretching vibration accelerates ESDPT, but the excitation of the intermolecular bending vibration suppresses ESDPT by analyzing the bandwidths in the FE spectrum of $7AI_2$.[5] However, the present study reveals that the excitation of the bending vibration (1β) only slightly decreases the ESDPT rate, but it is prominent that the stretching vibration (1σ) increases the ESDPT rate.

It should be noted that the ESDDT rate constant k_{PT}^{dd} exhibits a very large kinetic isotope effect (Table 1). However, the corresponding value measured in the condensed phase at room temperature is very different from the present result; the ratio k_{PT}^{hh}/k_{PT}^{dd} (=2−2.5)[6,12,14] is much smaller than the corresponding value of 710 obtained in this study. We infer that the population in the excited states involving the intermolecular vibrational mode predominantly contributes to the decay profiles observed in the condensed phase.

B. Kinetic Isotope Effects and Cooperativity of ESDPT. The ESDPT rate constant for $7AI_2$-*hh* cannot be estimated from the DF spectrum in Figure 4a, because the normal dimer fluorescence is absent due to the fast ESDPT. Alternatively, we estimate the ESDPT rate constant for $7AI_2$-*hh* from the width of the origin band in the FE spectrum. Figure 7 shows an enlarged feature of the FE spectrum of $7AI_2$-*hh*. The 0−0 band in Figure 7 is homogeneously broadened, and its bandwidth is ≈2.7 cm^{-1}, which is somewhat smaller than that (5.0 cm^{-1}) measured previously.[5] The relationship between the bandwidth and the lifetime is represented as

$$\Delta\tilde{\nu}_{FWHM} \approx \left(\frac{1}{2\pi c}\right)\cdot\frac{1}{\tau_{0-0}} \quad (5)$$

where τ_{0-0} is the lifetime of the zero-point level in the ^1B_u state of $7AI_2$-*hh*. The shape of the 0−0 band could be obtained by convoluting the excitation laser line shape (fwhm is about 0.2 cm^{-1}) and the homogeneous Lorentzian line shape of each rotational band. The lifetime obtained from the bandwidth in Figure 7 represents a lower limit of the lifetime. Because the quantum yield of the ESDPT reaction in $7AI_2$-*hh* is considered to be nearly unity,[12] the contribution of the radiative and the nonradiative decay processes other than ESDPT to the bandwidth of $7AI_2$-*hh* must be very small. From eq 5, we obtain $\tau_{0-0} \approx 2$ ps as a lower limit of the ESDPT time constant. The estimated ESDPT time constant for $7AI_2$-*hh* (2 ps) is nearly the average of a time constant (1.1 ps)[12] obtained by the femtosecond fluorescence up-conversion spectroscopy in the condensed phase and the slower decay component (3.3 ps) obtained by exciting the 0−0 region ($\Delta E \approx 0$kcal/mol) in the femtosecond pump−probe spectroscopy of $7AI_2$-*hh* in the gas phase.[8] Thus, we employ an ESDPT rate constant $\approx 5 \times 10^{11}$ s^{-1} ($\tau_{0-0} = 2$ ps) in order to roughly estimate the kinetic isotope effects on the ESDPT rate.

By comparing the k_{PT} values for the three $7AI_2$ dimers in Table 1, one can identify large kinetic isotope effects on the ESDPT rate: $k_{PT}^{hh}/k_{PT}^{hd} \approx 60$, $k_{PT}^{hd}/k_{PT}^{dd} \approx 12$, and $k_{PT}^{hh}/k_{PT}^{dd} \approx 710$, where k_{PT}^{hd} is approximated by $(k_{PT}^{h*d} + k_{PT}^{hd*})/2$. The estimated reaction rates may contain some errors originating from the ESDPT rate constant from the bandwidth in the FE spectrum and the calculations in eq 4 with the rate constants that are measured in the condensed phase. However, the prominent kinetic isotope effects on the reaction rate suggests that the first deuterium substitution strongly influences the reaction rate as compared with the second deuterium substitution; i.e., a prominent *asymmetric kinetic isotope effect* is found. It should be noted that k_{PT}^{dd} is nearly 3 orders smaller than k_{PT}^{hh}. We infer that an electronic reorganization occurs accompanying with the proton and deuteron transfers. The changes in the electron densities in the proton and deuteron acceptor sites may play an important role in the proton and deuteron transfer dynamics. In the case of $7AI_2$-*hd*, the change in the electron density in the proton acceptor site must be slow, because the deuteron transfer is much slower than the proton transfer. The H/D kinetic effects suggest that the motions of two transferring protons (or deuterons) couple each other through the electron motions; i.e., the ESDPT reaction of $7AI_2$ has a *cooperative* nature.

C. Effect of Localization and Excitation and ESDPT in $7AI_2$-*hd*. The k_{PT}^{hd} values are different between $7AI_2$-*h*d* and $7AI_2$-*hd**: $(9.8 \pm 0.6) \times 10^9$ s^{-1} for $7AI_2$-*h*d* and $(6.9 \pm 1.1) \times 10^9$ s^{-1} for $7AI_2$-*hd**. It is difficult to explain the different k_{PT} values for $7AI_2$-*h*d* and $7AI_2$-*hd** with a one-dimensional potential along the reaction coordinate. The $7AI_2$-*h*d* and $7AI_2$-*hd** have a common zero-point level in the S_0 state, whereas $7AI_2$-*hd** has larger zero-point energy than that of $7AI_2$-*h*d* in the S_1 state.[18] In the one-dimensional model, the k_{PT}^{hd} value may be larger for $7AI_2$-*hd** than for $7AI_2$-*h*d*, because the potential energy barrier height and the width of the barrier should be smaller for $7AI_2$-*hd** than for $7AI_2$-*h*d* due to the difference in the zero-point energies in the S_1 state. Therefore, the one-dimensional model cannot elucidate the larger k_{PT}^{hd} value for $7AI_2$-*h*d* than for $7AI_2$-*hd**. To explain the difference in the k_{PT}^{hd} values between $7AI_2$-*h*d* and $7AI_2$-*hd**, a multidimensional model is necessary.

The dual fluorescence from $7AI_2$-*h*d* and $7AI_2$-*hd** provides insight into the mechanism of ESDPT. The following scheme is assumed in the stepwise mechanism,

$$\text{normal dimer} \xrightarrow{k_1} \text{intermediate} \xrightarrow{k_2} \text{tautomer} \quad (6)$$

where k_1 and k_2 indicate the single-proton (or deuteron) transfer rate constants.[8,13] A stable intermediate dimer should exist in the stepwise mechanism. In this scheme, k_1 may exhibit very large kinetic isotope effect in $7AI_2$-*hd**, because the excitation is localized in the 7AI-*d* moiety, so that the deuteron transfer should occur before the proton transfer. In contrast, k_2 should show a large kinetic isotope effect in $7AI_2$-*h*d*. Therefore, the intensity ratio of the normal dimer fluorescence to the tautomer fluorescence of $7AI_2$-*hd** must be much larger than that of $7AI_2$-*h*d*. However, the ratio *I*(normal)/*I*(tautomer) is only 1.4 times larger for $7AI_2$-*hd**. The observed small isotope effect implies that the ESDPT reaction may occur via the concerted mechanism rather than the stepwise mechanism.

Conclusion

We have measured the DF spectra of $7AI_2$-*hh*, $7AI_2$-*h*d*, $7AI_2$-*hd**, and $7AI_2$-*dd*. Dual fluorescence has been observed in the spectra of $7AI_2$-*h*d*, $7AI_2$-*hd**, and $7AI_2$-*dd*. By determining the intensity ratios of the normal dimer fluorescence to the tautomer fluorescence excited at the origin bands, we have estimated the ESPDT and ESDDT rates for $7AI_2$-*h*d*, $7AI_2$-*hd** and $7AI_2$-*dd*. The ESDDT rate for $7AI_2$-*dd* excited at the origin is much smaller than those measured in the condensed phase. We have observed remarkable H/D kinetic isotope effects on the ESDPT reaction. It has been found that the H/D kinetic isotope effects, $k_{PT}^{hh}/k_{PT}^{hd} \approx 60$ and $k_{PT}^{hd}/k_{PT}^{dd} \approx 12$, are asymmetric. This observation suggests that the motions of the two protons couple each other through the electron motions. Thus, the ESDPT reaction in $7AI_2$ has a *cooperative* nature. The ESPDT rates are different between $7AI_2$-*h*d* and $7AI_2$-*hd**; the difference could be explained by considering the multidimensional proton/deuteron tunneling mechanism. The observed kinetic isotope effects are consistent with the concerted mechanism rather than the stepwise mechanism.

Acknowledgment. We thank Prof. M. Tsuji (Kyushu Univerisity) for allowing us to use a halogen lamp. This work was supported in part by the Grant-in-Aid for Scientific Research No. 15250015 from the Japanese Ministry of Education, Science, Sports and Culture.

References and Notes

(1) (a) Taylor, C. A.; El-Bayoumi, M. A.; Kasha, M. *Proc. Natl. Acad. Sci. U.S.A.* **1969**, *63*, 253. (b) Ingham, K. C.; Abu-Elgheit, M.; El-Bayoumi, M. A. *J. Am. Chem. Soc.* **1971**, *93*, 5023. (c) Ingham, K. C.; El-Bayoumi, M. A. *J. Am. Chem. Soc.* **1974**, *96*, 1674.

(2) Hetherrington, W. M., III; Micheels, R. H.; Eisenthal, K. B. *Chem. Phys. Lett.* **1979**, *66*, 230.

(3) Bulska, H.; Grabowski, A.; Pakula, B.; Sepiol, J.; Waluk, J.; Wild, U. P. *J. Lumin.* **1984**, *29*, 65.

(4) (a) Tokumura, K.; Watanabe, Y.; Itoh, M. *Chem. Phys. Lett.* **1984**, *111*, 379. (b) Tokumura, K.; Watanabe, Y.; Udagawa, M.; Itoh, M. *J. Am. Chem. Soc.* **1987**, *109*, 1346.

(5) (a) Fuke, K.; Yoshiuchi, H.; Kaya, K. *J. Phys. Chem.* **1984**, *88*, 5840. (b) Fuke, K.; Kaya, K. *J. Phys. Chem.* **1989**, *93*, 614.

(6) Share, P.; Pereira, M.; Sarisky, M.; Repinec, S.; Hochstrasser, R. M. *J. Lumin.* **1991**, *48/49*, 204.

(7) Chen, Y.; Rich, R. L.; Gai, F.; Petrich, J. W. *J. Phys. Chem.* **1993**, *97*, 1770.

(8) Douhal, A.; Kim, S. K.; Zewail, A. H. *Nature* **1995**, *378*, 260.

(9) Douhal, A.; Guallar, V.; Moreno, M.; Lluch, J. M. *Chem. Phys. Lett.* **1996**, *256*, 370.

(10) Nakajima, A.; Hirano, M.; Hasumi, R.; Kaya. K.; Watanabe, H.; Carter, C. C.; Williamson, J. M.; Miller, T. A. *J. Phys. Chem. A* **1997**, *101*, 392.

(11) Lopez-Martens, R.; Long, P.; Sogaldi, D.; Soep, B.; Syage, J.; Millie, P. *Chem. Phys. Lett.* **1997**, *273*, 219.

(12) (a) Takeuchi, S.; Tahara, T. *Chem. Phys. Lett.* **1997**, *277*, 340. (b) Takeuchi, S.; Tahara, T. *J. Phys. Chem. A* **1998**, *102*, 7740. (c) Takeuchi, S.; Tahara, T. *Chem. Phys. Lett*. **2001**, *347*, 108.

(13) (a) Folmer, D. E.; Poth, L.; Wisniewski, E. S.; Castleman Jr., A. W. *Chem. Phys. Lett.* **1998**, *287*, 1. (b) Folmer, D. E.; Wisniewski, E. S.; Castleman Jr., A. W. *Chem. Phys. Lett.* **2000**, *318*, 637.

(14) Chachisvilis, M.; Fiebig, T.; Douhal, A.; Zewail, A. H. *J. Phys. Chem. A* **1998**, *102*, 669.

(15) Mente, S.; Maroncelli, M. *J. Phys. Chem. A* **1998**, *102*, 3860.

(16) Guallar, V.; Batista, V.; Miller, W. H. *J. Chem. Phys*. **1999**, *110*, 9922.

(17) Fiebig, T.; Chachisvilis, M.; Manger, M.; Zewail, A. H.; Douhal, A.; Garcia-Ochoa, I.; De la Hoz Ayuso, A. *J. Phys. Chem. A* **1999**, *103*, 7419.

(18) Sakota, K.; Hara, A.; Sekiya, H. *Phys. Chem. Chem. Phys.* **2004**, *6*, 32.

(19) (a) Catalan, J.; Kasha, M. *J. Phys. Chem. A*, **2000**, *104*, 10812. (b) Catalan, J.; Perez, P.; del Valle, J. C.; de Paz, J. L. G.; Kasha, M. *Proc. Natl. Acad. Sci. U.S.A.* **2004**, *101*, 419.

(20) Sekiya, H. Atom Tunneling and Molecular Structure. In *Atom Tunneling Phenomena in Physics, Chemistry and Biology*; Miyazaki, T., Ed.; Springer: Berlin, 2004.

(21) El-Bayoumi, M. A.; Avouris, P.; Ware, W. R. *J. Chem. Phys.* **1975**, *62*, 2499.

(22) (a) Fulton, R. L.; Gouterman, M. *J. Chem. Phys*. **1961**, *35*, 1059. (b) Fulton, R. L.; Gouterman, M. *J. Chem. Phys.* **1964**, *41*, 2280.

(23) McRae, E. G.; Siebrand, W. *J. Chem. Phys.* **1964**, *41*, 905.

(24) Kanamaru, N. *J. Mol. Spectrosc*. **2004**, *225*, 55.

(25) Sakota, K.; Sekiya, H. *J. Phys. Chem. A* **2005**, *109*, 2718.

(26) Sakota, K.; Nishi, K.; Ohashi, K.; Sekiya, H. *Chem. Phys. Lett*. **2000**, *322*, 407.